Balkh International Journal of Natural Science

ISSN – P 0000 -0000 E: 0000- 0000
Vol.1 NO.2 2025
URL: https://bjns.ba.edu.af/index.php/bjns

The Problem of Extracting Transit Times from Transient Current Signals of Diamond Detectors in TCT Experiments

AUTHORS: Faiz Rahman Ishaqzai [1], Mohammad Ismail Ihsas [2], Rahmatullah Afghan [3]

1. TU Dortmund University, Germany
2.Teaching Assistant , Department of Physics, Faculty of Education Balkh University, Mazar-e-Sharif, Afghanistan.
3.Teaching Assistant , Department of Physics, Faculty of Education Helmand University, Helmand,Afghanistan.

Corresponding Author Name:Faiz Rahman Ishaqzai,Germany

Received: 21/1/2026 Accepted: 7/6/2026 Published: 19/7/2026

ABSTRACT

Transient-current technique (TCT) measurements are widely used to determine charge-transport parameters in single-crystal and polycrystalline CVD diamond detectors. In the space-charge-limited regime, however, the time coordinate of a waveform feature cannot, in general, be identified directly with the physical carrier transient time. This work analyzes the conditions under which an extraction-feature time may be converted into a drift transit time by means of a correction factor. We argue that the correction factor is not a universal constant for diamond detectors, but a configuration-dependent quantity governed by injected-charge density, optical absorption depth, pre-existing effective space charge, contact physics, surface termination, and polarization driven by trapping. These effects modify the internal electric field during the transit and shift commonly used timing

[1] Email: faiz.ishaqzai@tu-dortmund.de
ORCID iD:0009-0005-8577-8747
[2] Email: ihsas.ismail786@gmail.com
ORCID iD:0009-0003-8266-2218
[3] Email: rafgha7688@gmail.com
ORCID iD:0009-0005-8399-3689

markers, including cusp, kink, arrival-edge, and integrated-charge definitions. Treating the correction factor as a fixed numerical value may therefore introduce systematic errors in extracted mobilities, especially when the transient evolves from the space-charge-free to the space-charge-limited regime. We propose that mobility extraction from SCL-TCT waveforms should be based on explicitly defined timing markers, intensity-dependent diagnostic scans, and configuration-specific calibration through forward modelling or independently constrained field profiles. The analysis provides a practical framework for improving the reliability of transport-parameter extraction in diamond radiation detectors.

Keywords: Absorption profile, Contact polarization, Current technique, Currenttechnique, Diamond detectors, field,Redistribution.

1.INTRODUCTION

اَلْحَمْدُ للهِ رَبِّ العَالَمِينَ وَالصَّلاَةُ وَالسَّلَامُ عَلى سَيِدِالْمُرْسَلِينَ وَعَلَى اَلِهِ وَصَحْبِهِ اَجْمَعِينَ.

Single-Crystal CVD diamond combines high breakdown strength, radiation hardness, thermal stability, and fast charge transport, making it one of the most attractive wide-bandgap materials for radiation detection in high-rate and harsh environments. Early TOF measurements in intrinsic CVD diamond reported exceptionally high low-field mobilities, but also made clear that the space-charge-limited transit regime requires correction factors because the internal field is no longer spatially uniform during the transit [Isberg et al., 2002]. Subsequent work demonstrated that apparent mobility values may depend on the measurement mode, excitation density, illumination profile, and electrode or surface preparation [Nesládek et al., 2008]. In parallel, alpha-TCT measurements revealed that detector-grade diamond can contain net effective space charge, leading to non-rectangular electric-field profiles and strongly modified current pulses [Pernegger et al., 2005]. Recent mobility reviews and modelling studies further show that the excitation source, field window, and selected drift-velocity parameterization can produce systematic differences in extracted transport parameters [Ishaqzai et al., 2026].

A central methodological question is whether a space-charge-limited extraction feature, such as a cusp or kink in the transient current signal, can be converted into a physical transient time by applying a single numerical correction factor. Such a procedure is attractive because it is simple and can increase sensitivity at low electric fields, where small-signal TCT amplitudes are weak. Its validity, however, requires restrictive assumptions: a known

generation profile, negligible pre-existing space charge, stable contact boundary conditions, and a reproducible definition of the timing marker.

If these assumptions are not satisfied, the feature time is an observable of the full electrostatic relaxation process rather than a direct measure of carrier drift alone.

The purpose of this paper is therefore fourfold: (i) to clarify the distinction between waveform feature time and carrier transit time in SCLC/SCLT analysis; (ii) to show why the correction factor cannot be treated as a universal material constant for diamond; (iii) to connect absorption-profile effects, self-consistent field redistribution, bulk space charge, and contact polarization within a common physical picture; and (iv) to propose a practical workflow for extracting mobility and field-dependent transport parameters with explicit uncertainty budgets. The emphasis is not on changing the experimental format, but on improving the physical interpretation of timing markers used in diamond TCT and TOF measurements.

2.MATERIALS AND METHODS

2-1 Definitions and measurement regimes

2-1-1- SCF vs. SCL TCT signal

In a parallel-plate detector of thickness d biased at voltageU, the electrode charge scale is $\mathrm{Q}_0 = \mathrm{CU}$ (capacitanceC). TC signal is termed SCF when the generated charge$\mathrm{Q}_{\mathrm{ge}} \ll \mathrm{Q}_0$; in this regime the internal field remains approximately uniform and the drift transient time is commonly approximated by

$$t_T \simeq \frac{d^2}{\mu\, U}, \qquad (1)$$

For constant mobility and negligible field dependence. The SCL regime is entered when$Q_{\mathrm{ge}} \gtrsim Q_0$, where the drifting charge significantly redistributes $E(x,t)$ and waveform interpretation becomes nontrivial]Nesládek et al., 2008, Juška et al., 1994].

2-1-2- Timing markers: transient vs. extraction

In practice, TCT waveforms are analyzed by identifying a “feature time” such as, a) a kink or “cusp” in $J(t)$ (often in log-log plotting), b) the time at which the integrated charge reaches a fraction of its plateau, c) the onset of a falling edge associated with charge arrival (common in α-TCT). In SCL, it is common to define an *extraction time* t_E from the cusp and relate it to t_T by$t_E = \beta\, t_T$. Nesládek *et al.* explicitly reported that their experimentally

inferred β was about 0.85 while quoting a frequently used "theory" value near0.787, and suggested that contact-related field relaxation can shift β [Nesládek et al., 2008]. This observation alone signals that β is not a universal constant in realistic diamond structures.

2-1-3- Transition from space-charge-free (SCF) to space-charge-limited (SCL) transient currents

A central practical question is when a transient can be treated as *space-charge-free* (SCF) and when it becomes *space-charge-limited* (SCL). A convenient dimensionless injection-strength parameter compares injected (or photo-generated) charge to the electrode charge scale [Juška et al., 1994].

$$\Xi \equiv \frac{Q_{\mathrm{inj}}}{CU} \quad (2)$$

For $\Xi \ll 1$ the transient is expected to be SCF-like (the internal field is only weakly perturbed), whereas $\Xi \gtrsim 1$ indicates a strong likelihood of field redistribution and SCL-like waveform evolution. In diamond, the SCF→SCL transition has been demonstrated directly by scanning optical excitation intensity over orders of magnitude, showing that even comparatively small injected charge can affect drift-velocity extraction [Isberg et al., 2011]. This is consistent with broader modelling work emphasising that excitation source and the field window probed can bias extracted mobility parameterisations [Ishaqzai et al., 2026].

Diagnostic criterion and recommended plot. A robust experimental diagnostic is therefore an *intensity scan at fixed bias*, plotting an extracted timing marker (e.g.t_E, or a 50% arrival-time marker in α-TCT) versus Q_{inj} (or a calibrated proxy such as laser pulse energy). In SCF operation, the extracted timing marker remains stable and the amplitude scales linearly with Q_{inj}; in the transition regime, waveform shape and timing shift with Q_{inj}; in SCL, the timing feature becomes injection-dependent and may approach a space-charge-controlled shape [Many & Rakavy, 1962 , Juška et al., 1994 , Isberg et al., 2011].

3.RESULTS

3-1- Why a universal correction factor is problematic

Two independent physical mechanisms make a geometry-only correction factor unreliable in realistic diamond detectors:

1- Charge generation is not a delta-function sheet. Strongly absorbed particles/photons excitation generates carriers over a finite, often exponential, depth profile. This spatial profile couples to electrostatic screening and changes both the early-time field relaxation and the position of the observed cusp or kink [Juška et al., 1994].

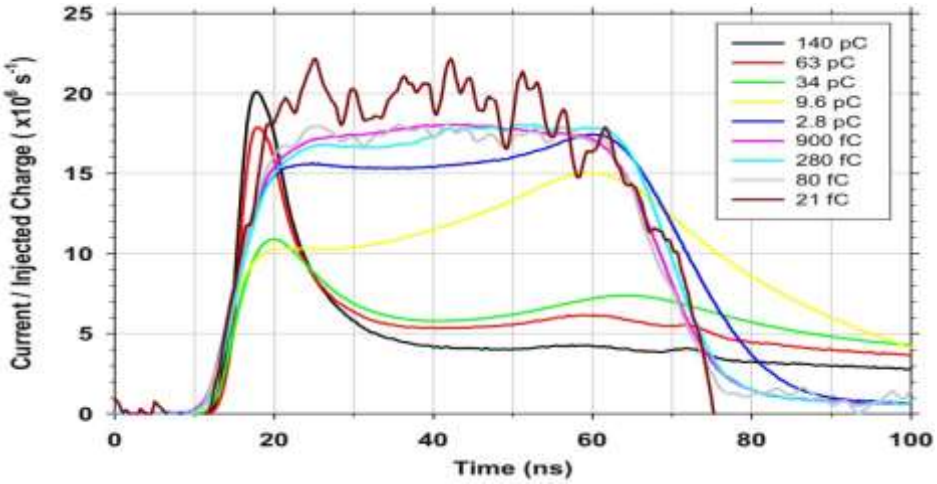

Figure1: Transient-current signal (holes) at 34 V for varying laser intensities, illustrating the transition from SCFC to SCLC currents at$Q_{inj} = 34pC$, figure adapted from [Isberg et al., 2011].

2- The internal electric field may be non-uniform even before injection. Bulk effective space charge, trapped charge, contact barriers, or surface states can produce a non-rectangular field profile. The drift velocity is then position dependent, and no single waveform feature can be mapped to a uniform-field transit time without an additional model [Nesládek et al., 2008, Pernegger et al., 2005].

These effects are independent and may coexist. For example, UV-laser TOF can combine shallow absorption with contact polarization, whereas alpha-TCT can combine a localized generation region with a pre-existing effective space charge. In both cases, the correction factor becomes a response parameter of the detector-measurement configuration.

3-2-Absorption-profile-controlled SCLC transients: transferable structure of the Juška model

Juška et al. developed a one-dimensional current-mode theory for space-charge-limited photocurrent transients in insulating photoconductors with blocking electrodes and a realistic exponential photogeneration profile

[Juška et al., 1994]. The important point for diamond detectors is not the microscopic material identity of the illustrative system, but the electrostatic structure of the problem: the waveform morphology is controlled by dimensionless parameters that describe injection strength, absorption depth, and boundary conditions.

Figure 2: Waveform taxonomy showing SCF and SCL transient currents for (a) holes, and (b) electrons. The figure is adapted from [Nesládek et al., 2008].

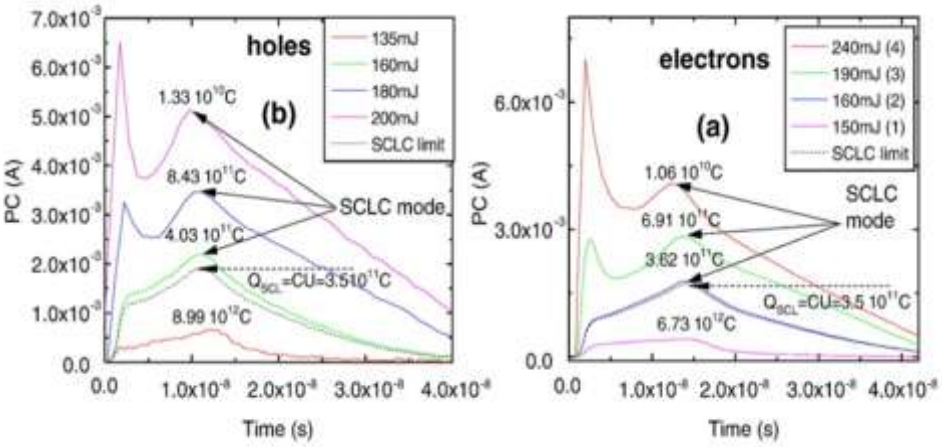

Figure 3: Signal degradation because of space charge buildup in Am-241 induced TCT experiment. The space-charge-build-up weakens the electric field a) for holes drift (left) and strengthens the electric field b) for electrons drift (right) [Pernegger et al., 2005].

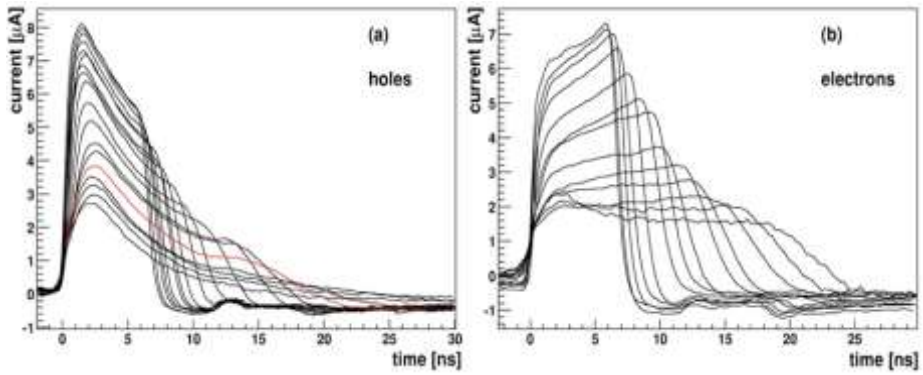

3-2-1- Normalization and governing equations

To compare transient-current waveforms obtained under different experimental conditions, the model of Juška et al [Juška et al., 1994]. can be written in dimensionless form. The position, time, and electric field are

normalized as $x' = x/d$, $t' = t/t_T$, and $E' = Ed/U$, respectively, where d is the detector thickness, U is the applied voltage, and $t_T = d^2/(\mu U)$ is the nominal transit time for carrier drift in a uniform electric field. In this formulation, the transient current is obtained from the self-consistent solution of the continuity equation, Poisson equation, and the constant-voltage boundary condition. A central result of this treatment is that the waveform is not determined only by mobility and applied bias, but also by the initial spatial distribution of photogenerated carriers. For finite optical absorption, the carriers are generated according to an exponential profile rather than as an ideal sheet, and this profile is governed by the dimensionless parameter αd. As a result, the electric field is rapidly screened near the illuminated electrode, the cusp position in the transient current is shifted, and an additional late-time feature may appear because some carriers remain temporarily localized near the generation region before being extracted. Therefore, the measured cusp time depends on excitation intensity and absorption depth in addition to mobility and voltage. This provides a direct physical reason why an extraction time in SCLC transients cannot, in general, be converted into a true transit time by using a universal correction factor κ [Juška et al., 1994].

3-2-2- Implications for β in diamond

In the standard idealized SCL transient picture, the cusp time approaches a constant fraction of t_T and is often associated with $\beta \simeq 0.78$ beyond the small-signal/SCF crossover. Juška *et al.* show that, once αd is finite and the injection is strong, the cusp time can continue to shift with intensity and may drop below the nominal $0.78\ t_T$ limit [Juška et al., 1994]. This mechanism is electrostatic and therefore transferable to diamond provided the measurement conditions satisfy the current-mode assumption and the relevant dimensionless parameters (notably Q_{ph}/Q_0 andαd) are comparable.

For diamond TOF measurements with UV excitation, Nesládek et al. reported an absorption depth of approximately 8 μm at a wavelength of 218 nm [Nesládek et al., 2008]. For a typical detector thickness of $d \sim 500$ μm, this corresponds to $\alpha d = d/\delta \sim 500/8 \approx 60$. Since αd is dimensionless, this indicates a strongly nonuniform photogeneration profile near the illuminated electrode. This is precisely the regime in which the Juška model predicts that the transient waveform and cusp time are sensitive to absorption geometry [Juška et al., 1994]. Therefore, even though diamond is a more ordered and less dispersive material than amorphous silicon, the timing markers in SCL measurements can still depend strongly on photogeneration geometry. A

universal correction factor κ should therefore not be assumed without configuration-specific calibration [Juška et al., 1994, Nesládek et al., 2008].

3-3- Correction factors from self-consistent modeling

Isberg *et al.* explicitly recognized that SCL produces an inhomogeneous field and therefore introduced a correction factor η for the TOF time scaling ,

$$\tau_{\mathrm{TOF}} = \eta \, \frac{d^2}{\mu U}, \qquad (3)$$

Stating that η depends on thickness and absorption profile and obtaining η by numerically solving the coupled transport–Poisson problem. They reported η values in the range $\approx$ 0.66–0.71 for their samples [Isberg et al., 2002]. This approach is conceptually more defensible than imposing a universalβ, because η is treated as an *experimental-configuration-dependent* correction rather than a constant of nature.

3-4- Bulk effective space charge and compensation voltage

Pernegger *et al.* analyzed α-TCT current pulses in single-crystal CVD diamond and showed that an approximately exponential increase (electrons) or decrease (holes) of the induced current can be explained by a net effective space charge in the bulk. In the simplest uniform-N_{eff} picture, Poisson's equation yields a linear field profile; the voltage needed to just compensate the space charge (so that the field extends across the full thickness) defines a *compensation voltage*V_c. The standard 1D relation is

$$V_c = \frac{e N_{\mathrm{eff}} d^2}{2\,\varepsilon_r \varepsilon_0} \quad \Leftrightarrow \quad N_{\mathrm{eff}} = \frac{2\,\varepsilon_r \varepsilon_0 V_c}{e d^2} \qquad (4)$$

Pernegger *et al.* extracted V_c and reported an average negative effective space-charge concentration of order10^{11} cm^{-3}, with indications of voltage dependence [Pernegger et al., 2005].

3-4-1- Consequences for TOF timing in SCLC/SCLT

If $E(x)$ is already non-uniform (or contains extended low-field regions) before optical injection, then a mapping between a single cusp time and a single uniform-field t_T becomes ill-defined. Even in small-signal operation, one should distinguish:

a. a *field-profile-dependent* drift time based on $\int_0^d x/(\mu E(x))$,
b. a *feature time* tied to a particular waveform definition (arrival edge, kink in $J(t)$, etc.) .

In SCLC operation, photoinjected space charge *adds* to the pre-existing N_{eff} and can further reshape$E(x,t)$, making any constant β correction especially fragile.

3-5- Contact and surface charge trapping

Nesládek *et al.* compared laser-TOF and α-particle TOF and emphasized that at low fields the extracted mobility can depend strongly on contact material and surface termination. They argued that time-dependent space charge building up due to trapping changes the internal field away from an ideal rectangular profile, shifting the apparent transit time. In the SCLC mode they observed a cusp and used $t_E = \beta t_T$ as a working relation, obtaining an experimental β of about 0.85 and attributing the deviation from the commonly quoted value to contact-related field relaxation and trapping [Nesládek et al., 2008].

This has two methodological implications:

1. A "universal" β cannot simultaneously account for differing contact physics across samples.
2. Even a calibrated β is not portable unless the surface/contacts and illumination profiles are matched .

3-5-1- Termination, passivation, and polarization as "hidden" space charge

Even when Q_{inj}kept small, transient waveform is can be modified by time-dependent internal fields arising from surface/interface states, contact barriers, or polarization (deep trapping under irradiation). High-k surface passivation has been shown to modify near-surface transport extracted by time-of-flight methods [Kovi et al., 2014]. Hydrogen/oxygen termination and surface isolation strategies can also impact detector performance through contact quality and surface conduction pathways [Su, Ren, Zhang, et al., 2020]. Polarization effects can cause rate-dependent signal degradation and effective space-charge build-up in diamond sensors [Kassel et al., 2017]. But mitigation strategies exist, including periodic forward-bias pulsing in diode configurations [Holmes, Dutta, Koeck, et al., 2019]. And direct microprobe studies of polarization and quenching dynamics [Rodríguez Ramos et al., 2022].

4- DISCUSSION

4-1- A non-universal correction β factor value

The preceding sections suggest that β should generally be treated as a function of a set of control parameters rather than as a constant :

$$\beta \equiv \beta\left(\underbrace{\frac{Q_{\mathrm{ph}}}{CU}}_{\text{injectionstrength}}, \underbrace{\alpha d}_{\text{absorptiondepth}}, \underbrace{\frac{\tau_{\mathrm{trap}}}{t_T}, \frac{\tau_{\mathrm{rec}}}{t_T}}_{\text{losses}}, \underbrace{\frac{V_c}{U}, N_{\mathrm{eff}}}_{\text{pre-existingspacecharge}}, \underbrace{\mathcal{B}}_{\text{boundary/contactphysics}}\right)$$

A constant β can be a reasonable *approximation* only in a restricted subset of conditions:

- negligible pre-existing space charge ($V_c \ll U$) ,
- negligible contact polarization/trapping on the transient timescale ,
- fixed and well-characterized αd ,
- moderate injection where the field redistribution follows the assumed idealized SCLT scenario ,
- a clearly specified, reproducible feature definition for t_E .

4-2- Physical interpretation of the correction factor

The correction factor should not be interpreted as a purely geometrical number. Its value reflects the self-consistent coupling between carrier drift, induced current, and the redistribution of the electric field inside the detector. In this sense, the correction factor is closer to a response parameter of the detector-measurement system than to a material parameter. A useful experimental test is the reproducibility of the factor under controlled changes of excitation intensity, bias voltage, wavelength, and contact condition. If the inferred value changes under these conditions, the measurement is not probing a universal transient-time relation but a configuration-specific electrostatic relaxation process.

A practical distinction should therefore be made between the feature time extracted from the waveform and the transient time used in mobility calculations. The feature time is experimentally defined; the transient time is model dependent. Reliable mobility extraction requires that the mapping

between the two be justified analytically, calibrated numerically, or validated experimentally. Modern mobility compilations and TCT/TCAD studies support this view because extracted parameters depend on source type, electric-field window, effective charge density, and boundary-condition modelling [Ishaqzai et al., 2026 , Kholili et al., 2024].

The relevant control parameters can be summarized as follows:

$$\eta = Q_{inj}/(CU), \quad \beta = \alpha L, \quad \nu = qN_{eff}L^2/(\varepsilon U),$$
$$\kappa = \kappa(\eta, \beta, \nu, \xi).$$

where η measures injected charge relative to the electrode charge, β is the normalized absorption parameter, ν measures the importance of pre-existing effective space charge, and ξ represents contact, surface, trapping, and polarization effects. This compact form emphasizes the central conclusion: κ is not a property of diamond alone, but of the complete measurement configuration. Low-density cyclotron-resonance and EBIC time-of-flight studies further demonstrate that mobility values are sensitive to carrier density, temperature, and measurement modality [Konishi et al., 2022 , Portier et al., 2023]. Polarization and high-temperature TCT studies show that trapped charge can distort transient traces and modify the internal field on experimentally relevant time scales [Zyablyuk et al., 2022 , Kraus et al., 2020].

Table 1. Physical origin of timing-marker shifts and their consequences for mobility extraction.

Effect	Physical origin	Consequence for feature time	Consequence for mobility
Large injected charge	Field screening and charge redistribution	Cusp or kink shifts with intensity	Apparent mobility becomes injection-dependent
Shallow absorption	Nonuniform generation profile	Effective drift length changes	Fixed correction factor becomes unreliable
Bulk space charge	Nonuniform pre-injection electric field	Arrival and extraction markers no longer map to uniform-field drift	Mobility becomes field-profile dependent
Contact polarization	Time-dependent boundary fields and surface states	Feature time shifts between samples or bias histories	Correction factor is not transferable

Effect	Physical origin	Consequence for feature time	Consequence for mobility
Trapping	Charge accumulation and delayed field relaxation	Signal degradation and delayed extraction features	Systematic over- or under-estimation of mobility

4-3- Recommended best-practice workflow for diamond

For reliable mobility extraction in diamond detectors, the transient-current analysis should be performed using a clearly defined and reproducible protocol. First, the transition between the space-charge-free and space-charge-limited regimes should be tested by varying the optical or particle-induced charge at fixed bias. In this test, the extracted timing marker should be plotted as a function of the injection-strength parameter $\eta = Q_{inj}/(CU)$, or of a calibrated experimental proxy such as laser pulse energy. A stable timing marker indicates approximately space-charge-free operation, whereas a systematic shift of the marker with injected charge indicates field redistribution and the onset of space-charge-limited behavior [Isberg et al., 2011 , Ishaqzai et al., 2026].

Second, small-signal TOF or TCT measurements should be used as the reference whenever possible. In this regime, the condition $Q_{ph} \ll CU$ should be satisfied, and the ratio Q_{ph}/CU should be explicitly reported [Juška et al., 1994, Nesládek et al., 2008]. Third, the optical absorption profile must be characterized by reporting the excitation wavelength, absorption depth, and the dimensionless absorption parameter αd, or equivalently $\beta = \alpha d$. If the absorption depth is not available from the literature, an attenuation measurement should be provided.

Fourth, the presence of bulk effective space charge should be checked using α-particle TCT, two-sided illumination, or another field-profile-sensitive method. When non-rectangular electric-field profiles are observed, the effective space-charge concentration N_{eff} and the compensation voltage V_c should be extracted where possible [4]. Fifth, contact and surface effects should be evaluated, particularly at low electric fields. Changes in waveform shape caused by different contact metals, surface terminations, or passivation conditions indicate that contact polarization or surface trapping contributes to the measured transient response [Nesládek et al., 2008, Kovi et al., 2014, Su, Ren, Zhang, et al., 2020].

Finally, when SCLC or SCLT waveforms are used for mobility extraction, the conversion between the extraction-feature time and the physical transit time should be calibrated by configuration-specific modelling. In this case, the correction factor κ should be obtained from self-consistent drift–

diffusion–Poisson simulations matched to the detector thickness, absorption profile, injected charge, bulk space charge, and boundary conditions, following the approach used by Isberg et al. [Isberg et al., 2002]. The definition of the timing marker must also be stated explicitly, for example whether t_E is determined from a cusp in J(t), a log–log slope change, a fixed fraction of the integrated charge, or an arrival-edge criterion. The final mobility uncertainty should include contributions from timing pickoff, detector thickness, applied voltage, absorption profile, and the model-dependent correction factor.

5.CONCLUSION

The analysis shows that the extraction-feature time in space-charge-limited transient-current measurements of diamond detectors is not, in general, a universal proxy for the carrier transit time. The apparent correction factor depends on the evolution of the internal electric field, which is controlled by injected charge, absorption profile, pre-existing effective space charge, and contact- or surface-related polarization. Consequently, a fixed correction factor may lead to systematic errors in mobility extraction when applied outside the conditions under which it was calibrated. A more reliable procedure is to define the timing marker explicitly, verify the space-charge-free or space-charge-limited character of the transient through intensity scans, and use configuration-specific modelling when field redistribution is significant. This distinction between waveform feature time and physical transit time is essential for obtaining reproducible charge-transport parameters in diamond detectors.

6. REFERENCES

Isberg, J., Hammersberg, J., Johansson, E., Wikstrom, T., Twitchen, D. J., Whitehead, A. J., & Scarsbrook, G. A. (2002). High carrier mobility in single-crystal plasma-deposited diamond. *Science*, *297*(5587), 1670-1672.

Holmes, J. M., Dutta, M., Koeck, F. A., Benipal, M. K., Hathwar, R., Brown, J., & Nemanich, R. J. (2019). Neutralizing the polarization effect of diamond diode detectors using periodic forward bias pulses. *Diamond and Related Materials*, *94*, 162-165.

Isberg, J., Gabrysch, M., Majdi, S., Kovi, K. K., & Twitchen, D. (2011). On the transition between space-charge-free and space-charge-limited conduction in diamond. *Solid state sciences*, *13*(5), 1065-1067.

Ishaqzai, F. R., Deniz, M., Kröninger, K., & Weingarten, J. (2026). Review and modelling of charge carrier mobility in diamond. *Diamond and Related Materials*, 113558.

Juška, G., Viliunas, M., Klíma, O., Šípek, E., & Kočka, J. (1994). New features in space-charge-limited-photocurrent transients. *Philosophical Magazine B*, *69*(2), 277-289.

Kassel, F., Guthoff, M., Dabrowski, A., & De Boer, W. (2017). Description of radiation damage in diamond sensors using an effective defect model. *physica status solidi (a)*, *214*(11), 1700162.

Kholili, M. J., Shimaoka, T., Hara, A., & Tanaka, M. M. (2024). Transient-Current Technique Characterization of Diamond Detector and Proposal of a Diamond Detector with Charge Amplification. *physica status solidi (a)*, *221*(4), 2300673.

Konishi, K., Akimoto, I., Matsuoka, H., Isberg, J., & Naka, N. (2022). Intrinsic Mobility of Low-Density Electrons in Photoexcited Diamond. *Physical Review Applied*, *17*(3), L031001.

Kovi, K. K., Majdi, S., Gabrysch, M., & Isberg, J. (2014). A charge transport study in diamond, surface passivated by high-k dielectric oxides. *Applied Physics Letters*, *105*(20).

Kraus, B., Steinegger, P., Aksenov, N. V., Dressler, R., Eichler, R., Griesmayer, E., ... & Weiss, C. (2021). Charge carrier properties of single-crystal CVD diamond up to 473 K. *Nuclear Instruments and Methods in Physics Research Section A: Accelerators, Spectrometers, Detectors and Associated Equipment*, *989*, 164947.

M. A. Lampert and P. Mark, (1979). *Current Injection in Solids* (Academic Press, New York,)**.**

Many, A., & Rakavy, G. (1962). Theory of transient space-charge-limited currents in solids in the presence of trapping. *Physical review*, *126*(6), 1980.

Nesladek, M., Bogdan, A., Deferme, W., Tranchant, N., & Bergonzo, P. (2008). Charge transport in high mobility single crystal diamond. *Diamond and Related Materials*, *17*(7-10), 1235-1240.

Pernegger, H., Roe, S., Weilhammer, P., Eremin, V., Frais-Kölbl, H., Griesmayer, E. ... & Whitehead, A. (2005). Charge-carrier properties in synthetic single-crystal diamond measured with the transient-current technique. *Journal of Applied Physics*, *97*(7).

Portier, A., Donatini, F., Dauvergne, D., Gallin-Martel, M. L., & Pernot, J. (2023). Carrier mobility up to 10^{6} cm^{2} V^{-1} s^{-1} measured in single-

crystal diamond by the time-of-flight electron-beam-induced-current technique. *Physical Review Applied*, *20*(2), 024037.

Rodríguez Ramos, M. R., et al. (2022). Ion microprobe study of the polarization quenching in single-crystal CVD diamond radiation detectors. *Sensors*, *22*.

Su, K., Ren, Z., Zhang, J., Liu, L., Zhang, J., Zhang, Y., & Hao, Y. (2020). High performance hydrogen/oxygen terminated CVD single crystal diamond radiation detector. *Applied Physics Letters*, *116*(9).

Xu, W., Wu, K., Wang, L., Xi, S., Huang, G., Wang, Z., ... & Liu, H. (2025). Research on the polarization effect and degradation of diamond detectors based on transient current technique. *Nuclear Instruments and Methods in Physics Research Section A: Accelerators, Spectrometers, Detectors and Associated Equipment*, 171162.

Zyablyuk, K., Popovich, A., Ralchenko, V., & Yurov, V. (2022). Polarization and depolarization control of single crystal CVD diamond detectors by UV and visible light illumination. *Nuclear instruments and methods in physics research section a: accelerators, spectrometers, detectors and associated equipment*, *1042*, 167461.